Final Report

Characterization of Corpus Christi and San Antonio Air Quality During the 2021 Ozone Season

AQRP Project 20-003

Submitted by

Robert Griffin, Rice University

James Flynn, University of Houston

Rebecca Sheesley, Baylor University

Sascha Usenko, Baylor University

Yuxuan Wang, University of Houston

August 31, 2021

Executive Summary

This report focuses on field work, data analysis, and modeling of air quality in Corpus Christi, in the area downwind (that is also upwind of San Antonio), and in San Antonio during the spring of 2021. Compared to other urban areas in Texas, these locations have received considerably less attention from the atmospheric science/air quality research community, despite issues related to their compliance with air quality regulations.

The platform for the field measurements was the University of Houston/Rice University/Baylor University Mobile Air Quality Laboratory 2 (MAQL2). The instrumentation on the MAQL2 includes sensors to measure meteorological parameters, inorganic trace gases that can be used as emissions tracers and that are relevant to both particulate matter and ozone formation (including carbon monoxide, carbon dioxide, nitrogen oxides, total reactive nitrogen, sulfur dioxide, and ozone itself), volatile organic compounds, and particulate matter composition, concentration and optical properties.

Quality assurance protocols were applied to the data generated by the MAQL2 instrumentation. After these efforts, the result was a time series of all measured parameters, which will allow investigation of the physical and chemical processes that contribute to the level of air pollutants at these locations.

These analyses were supplemented by three-dimensional air quality modeling using the Weather Research and Forecasting-GEOS Chem platform. Model output was compared to parameters measured by both the MAQL2 and the regional monitoring network; model runs were used to evaluate air pollution sensitivity to emissions scenarios.

Main observations include the importance of off-shore activities for determining the composition of air being transported into the Corpus Christi atmosphere, the importance of local activities on top of these off-shore activities in determining air quality in both Corpus Christi and San Antonio, and large differences in both composition and concentration of air pollutants across the spatial extent of the field campaign. Three-dimensional air quality modeling was able to simulate accurately the meteorology and air quality observations across the campaign once changes in background ozone and in emissions of anthropogenic combustion tracers were considered.

Table of Contents

List of Figures

List of Tables

Introduction

During the early part of the past decade, the sites that comprise the air quality monitoring network in the greater San Antonio metropolitan area exhibited at least one day per year on which the observed daily maximum eight-hour average ozone (O_3) mixing ratio exceeded 70 parts per billion by volume (ppbv), the value stipulated by the National Ambient Air Quality Standards (NAAQS), based on Texas Commission on Environmental Quality (TCEQ) data, which are publicly available online. Despite these observations, an assessment of published literature revealed very limited peer-reviewed research that elucidates the causes of enhanced O_3 mixing ratios in San Antonio. Thus, investigation of the physical and chemical processes that control O_3 formation in this region was warranted and provided the motivation for the San Antonio Field Study (SAFS), supported by TCEQ and its Air Quality Research Program (AQRP), that occurred in spring (May) 2017.

With respect to O_3, findings from the SAFS indicate that San Antonio was predominantly in a nitrogen oxide (NO_X)-limited regime, which led to a very high O_3 production efficiency, especially on days with relatively strong solar radiation. Compared to NO_X, O_3 formation in San Antonio was less sensitive to major volatile organic compounds (VOCs) such as alkanes, ethane, and acetone. Isoprene, formaldehyde (HCHO), and alkenes exhibited high reactivity (defined as the product of the species concentration and its rate coefficient for the reaction with hydroxyl radical). Local O_3 formation at San Antonio was driven both by organic peroxy radicals and the hydroperoxy radical, with a production rate peaking at mid-day.

The SAFS also included measurement of particulate matter (PM) because of the inextricable relationship between PM and trace gases relevant to O_3 formation (in terms of both co-emission and chemical interaction). Analyses of PM data from SAFS indicate that high sulfate plumes were mostly related to air masses coming from the Gulf of Mexico, which implied that the sulfate aerosol observed at San Antonio was less likely to be locally produced. Instead, the sulfate aerosols represented mostly a regional, background level which could be attributed to both biogenic marine sources and regional sulfate-related anthropogenic activities, including those in the Gulf of Mexico and potentially those in locations outside the United States. Additional PM analyses indicate the importance of secondary organic aerosol (SOA) formation over the San Antonio region and the lack of influence of wildfires and biomass burning in Central America on PM in San Antonio during SAFS.

A second urban area in Texas that suffers from relatively poor air quality (based on similar TCEQ data as those mentioned above for San Antonio) is Corpus Christi. Though smaller in population compared to San Antonio, Corpus Christi is home to much more significant infrastructure associated with the petrochemical industry; thus, the emission profiles of the two urban areas are quite different. The coastal location of Corpus Christi also causes its meteorology and the relevant atmospheric chemistry to be unlike those in San Antonio.

Based on current understanding, as described above, the relevant scientific questions asked for this project (and related hypotheses) are:

Question A: What is the nature of the air being transported into Corpus Christi from the Gulf of Mexico, and how does it compare to air being transported into Galveston/Houston? *Related Hypothesis:* Because of the anthropogenic activities occurring in the Gulf of Mexico and areas outside the United States, the air coming into Corpus Christi from the ocean (a predominant wind direction during O_3 season) will be polluted (in terms of sulfate aerosol, organic PM, and NO_X) compared to other coastal locations. However, because of the smaller port in Corpus Christi, the air transported into Corpus Christi will be less polluted than that

transported into Galveston, except when Corpus Christi is influenced directly by fire emissions from Central America.

Question B: What is the impact of local emissions on air quality as air is advected through Corpus Christi? *Related Hypothesis:* Within Corpus Christi itself, due to limited large tree vegetation, it will be anthropogenic activities, predominantly those associated with vehicular traffic, the port, and the petrochemical processing, that primarily drive emissions and influence chemistry. As with many urban areas, it is expected that the region will be NO_X-limited with respect to O_3 formation and that organic PM will be dominated by SOA.

Question C: What is the nature of the air being transported into San Antonio along the I-37 corridor, including potential contributions from Corpus Christi, the Gulf of Mexico, and locations outside the United States? *Related Hypothesis:* The change in air quality between Corpus Christi and San Antonio will be driven by phenomena including deposition, dispersion, emissions from local sources, and chemical processing. The emissions and chemistry associated with Corpus Christi will impact the regional background measured downwind.

To address these questions, the project was broken down into three tasks. The first two were preparation for and performance of a field campaign. The third task was data analysis, including application of three-dimensional (3D) modeling.

Methodology: Field Campaign

To address these scientific questions, a field project using a combination of stationary and mobile measurements was performed. Originally, the field portion of this effort was slated to occur during late summer of 2020; the COVID pandemic forced its postponement to spring of 2021. To ensure statistical significance through a large enough number of data points and that any temporal variability in air quality was captured, the following overall measurement timeline was followed.

- Weeks 1 and 2 (April 1 – April 14, 2021): Stationary measurements in a coastal Corpus Christi location;
- Week 3 (April 15 – 21, 2021): Perform daily mobile measurements downwind (to the northwest) of Corpus Christi;
- Week 4 (April 22-28, 2021): Perform mobile measurements upwind (to the southeast) of San Antonio;
- Weeks 5 and 6 (April 29 – May 12, 2021): Perform stationary measurements at a location near the core San Antonio area; and
- Week 7 (May 13 – 19, 2021): Perform mobile measurements downwind (to the northwest) of San Antonio.

The University of Houston (UH)/Rice University (RU)/Baylor University (BU) Mobile Air Quality Laboratory 2 (MAQL2) used to house the instrumentation that performed these measurements is comprised of a BU-owned trailer and a BU-owned truck to tow the equipment trailer. The trailer has a volume of ~22 m^3, which was sufficient for all of the equipment listed subsequently, as well as area for team members to work when the trailer is not in motion. Integrated into the insulated trailer is a 15,500 BTU air-conditioning system to help provide protection for the instrument and team members. The ambient trace gas sample air was drawn through an inlet box that houses valves, converters, and power supplies for sampler configuration

and calibration. The ambient aerosol is segregated by a 2.5-μm cyclone inlet and transmitted to the aerosol analytical instrumentation through a 3/8-in. copper tubing inlet. Additionally, the MAQL2 was equipped with wired and wireless network, dual 4G cellular internet connections. The truck that towed this trailer is a 2015 Ford F250. The truck and trailer were wired to distribute power from either a generator while in motion or from a 50-A recreational vehicle (RV) power outlet for stationary measurements.

The generator was carried in the bed of the truck. The inlet associated with the instrumentation was forward of the generator and truck exhaust to avoid self-sampling when in motion. When operating in stationary mode, the truck was placed facing into the wind (if it was strong enough), and an exhaust hose was used to increase the distance between the truck and generator exhaust and the sampling inlets. When wind was not strong enough, for extended periods of stationary measurements, the MAQL2 was transferred to utility power and the truck/generator was detached. A telescoping tower was attached to the trailer to allow sampling from a greater height when in stationary mode. The length of inlets from the trailer walls to the instruments was made as short as possible (0.5 m; ~3 sec); these lengths of tubing were insulated to minimize wall loss and vaporization effects associated with temperature changes between outside and inside the trailer.

The MAQL2 instrumentation measured multiple trace gases at sub-minute time scale, including O_3, nitric oxide (NO), nitrogen dioxide (NO_2) ($NO_X = NO + NO_2$), total reactive nitrogen (NO_y), carbon monoxide, carbon dioxide (CO_2), sulfur dioxide, and VOCs. Ozone was monitored using two instruments. One was a Thermo Environmental, Inc., Model 42C that has been modified to measure O_3 via chemiluminescence (CL) with NO gas, and the other was an ultraviolet absorption instrument (2BTechnologies, Inc., Model 205). In Corpus Christi, the NO_X species were measured using an Air Quality Designs (AQD), Inc., high-sensitivity NO_X instrument, using CL to detect NO and photolysis and CL to measure NO_2. Due to several issues in the field, the AQD NOx instrument was replaced in San Antonio on April 23, 2021 with two NO and NO_2 CL instruments (Thermo Environmental, Inc., Model 42C). The NO_y was measured with a molybdenum oxide catalytic converter inlet and subsequent CL (Thermo Environmental, Inc., Model 42i). Carbon monoxide was measured using off-axis integrated cavity output spectroscopy (Los Gatos Research, Inc., CO-23R). Sulfur dioxide was measured using a pulsed fluorescence analyzer (Thermo Environmental, Inc., Model 43C). Carbon dioxide was measured using infrared absorption (LiCor Li-7000). A unit-mass resolution, proton-transfer reaction-mass spectrometer (PTR-MS) measured VOCs while operating in full-scan mode from mass-to-charge ratio (m/z) 21 to m/z 140. Operation in this manner allows for detection of HCHO (m/z 31) (which requires the appropriate sample conditioner), acetonitrile (m/z 42), acetaldehyde (m/z 45), acetone (m/z 59), isoprene (m/z 69), methyl vinyl ketone plus methacrolein (m/z 71), benzene (m/z 79), toluene (m/z 93), styrene (m/z 105), C_2-alkylbenzenes (m/z 107), C_3-alkylbenzenes (m/z 121), C_4-alkylbenzenes (m/z 135), and monoterpenes (m/z 136).

The chemical composition of non-refractory sub-micron PM was measured with an Aerodyne high-resolution time-of-flight aerosol mass spectrometer (HR-ToF-AMS). The species quantified by the HR-ToF-AMS include sulfate, nitrate, chloride, ammonium, and organic PM. Aerosol optical properties (absorption and scattering) were measured using a Brechtel model 2091 tri-color absorption photometer (TAP) and a TSI model 3563 nephelometer. These measurements provide data for absorption coefficient (σ_{abs}) and scattering

coefficient (σ_{scat}). These allow calculation of the absorption Ångström exponent (AAE), scattering Ångström exponent (SAE), and single scattering albedo (SSA).

Measurements of meteorological parameters (temperature, relative humidity, wind speed and direction, and pressure) and NO_2 photolysis rate (j_{NO2}) were performed at the trace gas inlet. Wind speed and direction were measured using a RM Young 86000 ultrasonic anemometer and Airmar Weather Station 200WX. Reported wind speed and wind direction from Mustang Beach Airport (approx. 1 km SE of stationary site) is included in the wind dataset during stationary periods at Corpus Christi due to issues with the RM Young ultrasonic anemometer. An RM Young 41382 temperature and relative humidity probe and a 61302V barometric pressure sensor was used. A Meterologie Consult, GmbH filter radiometer measured j_{NO2}. In addition, a Vaisala CL-31 determined planetary boundary layer height.

Quality assurance/control (QA/QC) protocols described in the Quality Assurance Project Plan (QAPP) submitted as part of this work were followed. As a result of these QA/QC protocols, minimum detection limits for all pollutant instrumentation were determined. They are summarized in Tables 1-3.

Table 1. Minimum detection limit (MDL) for 30-s averaged data and associated uncertainty for trace gas measurements including carbon monoxide (CO), carbon dioxide (CO_2), nitric oxide (NO), nitrogen dioxide (NO_2), reactive nitrogen oxides (NO_y), ozone (O_3) and sulfur dioxide (SO_2). NO, NO_2, and O_3 are distinguished by either instrument (Thermo, AQD, 2B Tech) or modification (CL) type.

Species	***Uncertainty (%)***	***MDL (ppbv)***
CO	1.4	0.13
CO_2	1.0	0.33
NO (AQD)	4.7	0.07
NO (Thermo)	4.5	0.35
NO_2 (AQD)	5.4	0.13
NO_2 (Thermo)	9.3	0.49
NO_y	5.6	0.48
O_3 (CL)	1.9	0.23
O_3 (2B)	3.5	1.30
SO_2	9.1	0.92

Table 2. Minimum detection limit (MDL) in ppbv and uncertainty associated with the measured VOCs during the sampling campaign. DMS = dimethyl sulfide; MVK = methyl vinyl ketone; MACR = methacrolein; MEK = methyl ethyl ketone. Note that the PTR-MS is unable to distinguish between MVK and MACR, both of which are oxidation products of isoprene.

Species	***m/z***	***Uncertainty (%)***	***MDL***
HCHO	31	10.8	0.66
Acetonitrile	42	10.7	0.09
Acetaldehyde	45	9.6	0.26
Acetone	59	20.9	0.42
DMS	63	9.6	0.15
Isoprene	69	10.1	0.15
MVK+MACR	71	9.5	0.16
MEK	73	9.6	0.12
Benzene	79	9.9	0.13
Toluene	93	9.9	0.16
Monoterpene	137	11.2	0.52
Hydroxyacetone	75	16.7	0.44
Styrene	105	11.4	0.10
Xylene	107	11.1	0.18

Table 3. The 1-min and 2.5-min detection limits (DL) of the measured nonrefractory submicron aerosol species during the sampling campaign, which were determined as three times the standard deviation (3σ) of the corresponding signals in particle-free ambient air.

Species	**DL - 1 min (μg m^{-3})**	**DL - 2.5 min (μg m^{-3})**
Organics	0.279	0.370
Sulfate	0.077	0.072
Nitrate	0.027	0.020
Ammonium	0.044	0.063
Chloride	0.030	0.024

For many of the instruments (trace inorganic gases, meteorological parameters, etc.) listed above, output provide time series of measured parameters, once QA/QC protocols described in the project QAPP are followed. The same is true for calculated properties such as the SSA. However, data collected by the PTR-MS and HR-ToF-AMS require more significant processing (beyond blank correction) to produce time series.

For the HR-ToF-AMS, first, a time- and composition-dependent collection efficiency (CE)

must be applied to all data in order to account for particle loss in the inlet and instrumentation. All data shown here have been corrected using this method, leading to an average (±1σ) CE of 0.46 (±0.04). Second, despite the fact that the HR-ToF-AMS operates under vacuum, the high level of atmospheric CO_2 can interfere with the signal at m/z 44 in the particle mass spectrum. Thus, time-dependent gas phase CO_2^+ subtraction was performed to remove this interference and to improve the determination of organic aerosol (OA) mass concentration and mass spectra. Measurements of CO_2 were used. Figure 1 shows both the time series of OA attributed to m/z 44 (top) and total organic aerosol (bottom), along with the time series of CO_2 (in parts per million by volume, ppmv), for both the default correction and the correction using ambient CO_2 measurements. While only minimal differences are observed, all data presented in the remainder of this report represent ambient-corrected data.

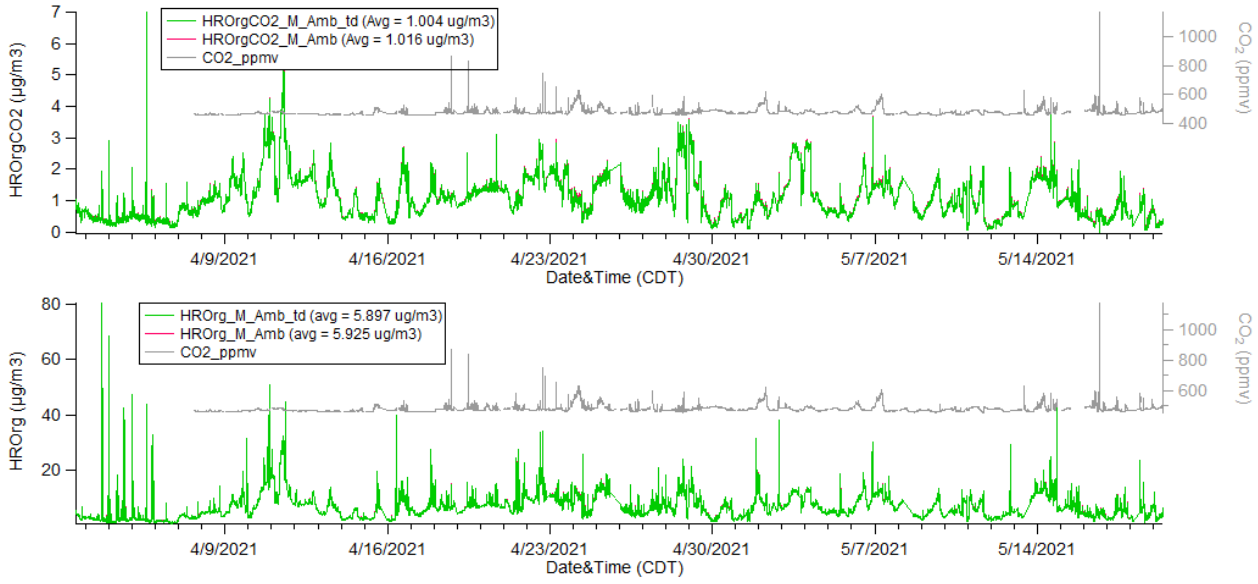

Figure 1. Time series of CO_2^+ mass concentration at m/z 44 resulting from particulate organics ($HROrgCO_2$; top panel) and total organic aerosol mass concentration (HROrg; bottom panel) derived from the default treatment of interference from gaseous CO_2 – subtracting a constant CO_2^+ signal at m/z 44 assuming constant gaseous CO_2 - versus an updated treatment – subtracting a time-dependent CO_2^+ signal based on the measured gaseous CO_2 mixing ratio. Time-dependent CO_2 subtraction made a small difference for some periods, and on average, organic mass at m/z 44 and total organic mass decreased by 0.014 µg m^{-3}.

The final process that needs to be considered for HR-ToF-AMS data is a comparison of time series using unit mass resolution (umr) mass spectral data and that using HR mass spectral data. The umr data provide greater signal and thus decreased uncertainty. The HR data provide greater insight into the ions that contribute to mass at each m/z value and thus properties such as molecular composition. Figure 2 shows time series for both the umr and HR data for the five main PM constituents measured by the HR-ToF-AMS. Tight correlations between speciated aerosol mass estimated using umr data and those using HR provide support for use of HR data.

Thus, all HR-ToF-AMS data shown in the remainder of this report reflect HR mass spectra and include correction for blanks, CDCE, and ambient CO_2 interference.

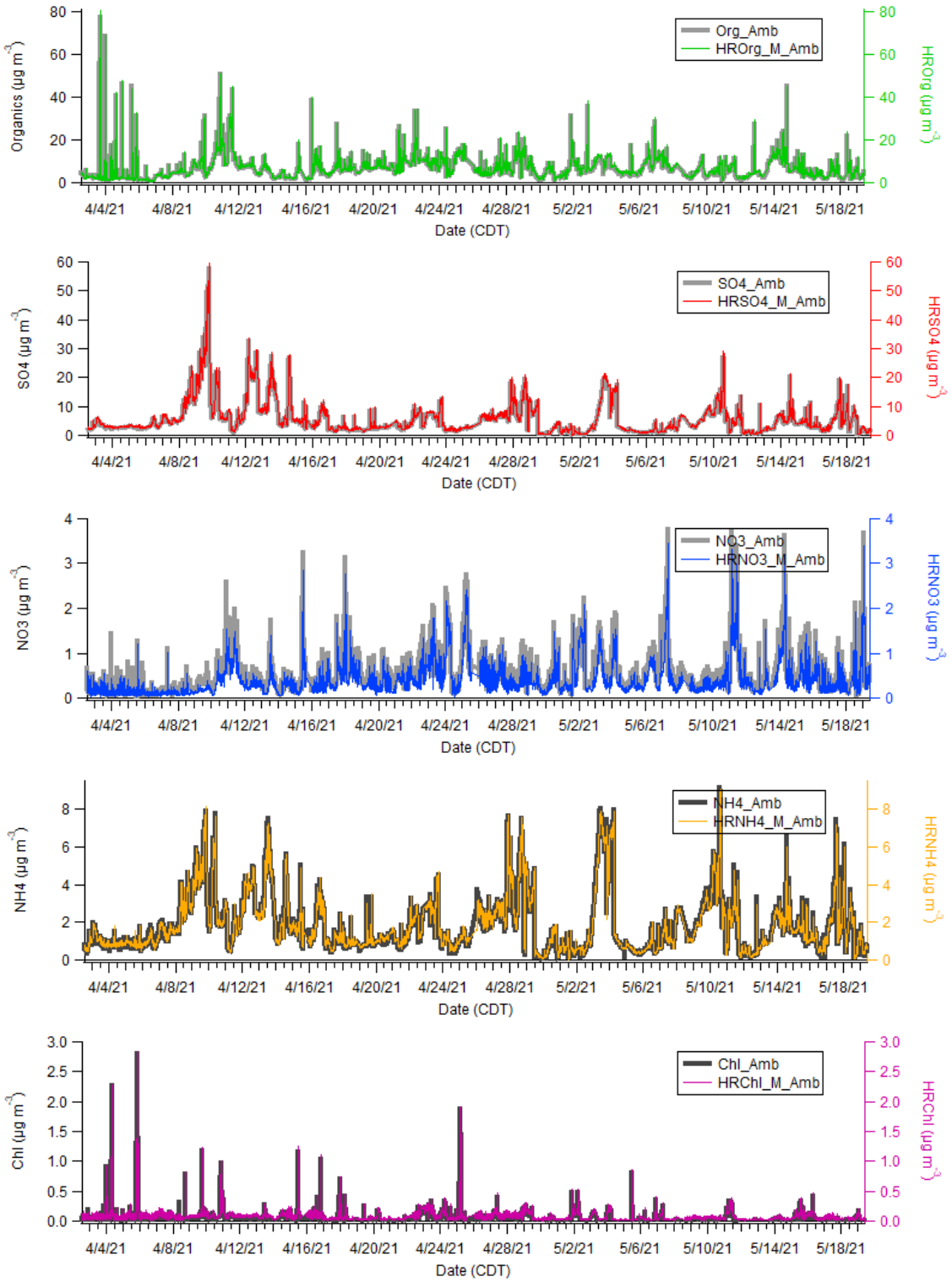

Figure 2. Time series of non-refractory submicron aerosol species obtained from the umr analysis (left axes) and HR analysis (right axes) for the entire sampling period.

In addition to generating time series of bulk organic aerosol using HR-ToF-AMS data, positive matrix factorization (PMF) is utilized to deconvolve the total organic aerosol into several aerosol types that constitute organic aerosol. In short, PMF is a statistical technique that minimizes residuals between simulated and observed time series and average mass spectra assuming linear combination of several types of organic aerosol and constant mass spectra for the factors. Using PMF, total organic aerosol can be broken down into organic aerosol factors that describe its sources (e.g., biomass burning) or its characteristics (e.g., more oxidized or less oxidized, hydrocarbon-like).

Methodology: Modeling

A multi-scale modeling framework that uses the Weather Research and Forecasting (WRF) meteorology model to drive the GEOS-Chem chemical transport model, named WRF-GC, was utilized. This modeling framework is a new capability of the GEOS-Chem chemical transport model that has been applied successfully by the project team to interpret SAFS 2017 field measurement data and simulate long-range transport of fire emissions from Central America to Corpus Christi and Houston.

The WRF has a powerful and flexible grid system, including multiple nested grids and moving nested grids. For this work, the inner-most model domain of WRF-GC was at a resolution of 1 km x 1 km. The advantage of fine-resolution meteorology that comes with WRF allowed replication of fine-scale temporal and spatial dynamics specific to coastal regions such as a sea/bay breeze. The model domain and information about grid sizes are included in Figure 3. The GEOS-Chem model has a state-of-the-science, well-documented, and benchmarked chemical module that fully couples gas and aerosol chemistry, including the recent development of halogen chemistry, which is of particular utility for coastal environments. Combining the advantages of the two models, WRF-GC allowed simulation of the chemical and dynamical complexity of the field measurements.

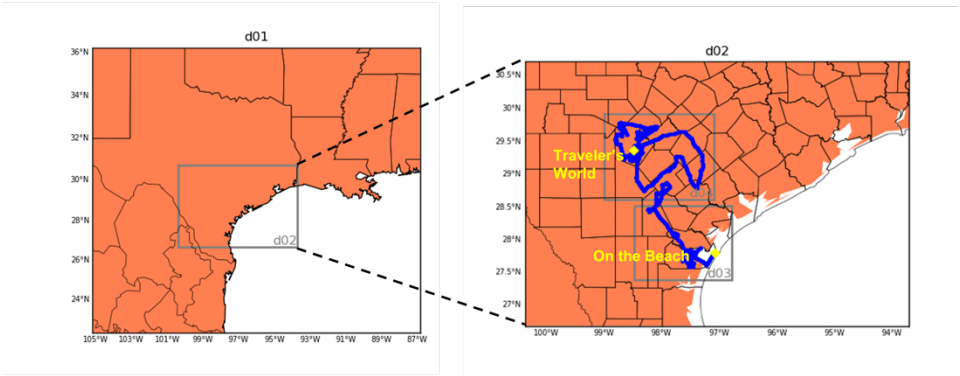

	Region	Horizontal Resolution	Domain Size	Output frequency
Domain 1	Texas	25 km	73 × 64	6-hourly
Domain 2	Southeast Texas	5 km	131 × 91	3-hourly
Domain 3	Corpus Christi	1 km	166 × 126	hourly
Domain 4	San Antonio	1 km	186 × 146	hourly

Figure 3. Nest-grid WRF-GC model domains, with each domain represented by d0n with n being described in the table below the maps. Stationary sampling locations are marked with the white diamond in the right-hand map.

The emissions inventory used reflects year-2011 National Emission Inventory data scaled to year 2013 for the United States and year-2014 Community Emission Data System information for the rest of the world. Biogenic emissions are from the Model of Emissions of Gases and Aerosols from Nature, and soil and lightning NO_x emissions are included.

Results Task 1 – Campaign Preparation

Task 1 focused on logistics, preparation of the MAQL2 for deployment, and maintenance and calibration of instrumentation prior to uploading to the MAQL2. It also involved training of staff from all three institutions. Logistics included determination of the location of the stationary sites, identification and reservation of appropriate lodging for staff in the field, and planning of mobile sampling routes for relevant portions of the campaign. Preparation of the MAQL2 included ordering and installing parts, ensuring that the trailer and truck had adequate power, shock absorption, and air conditioning to allow sampling while in motion, and designing and installing the inlets and sampling tower. All instrumentation were in working order and calibrated, and all staff were trained prior to the start of the campaign. Thus, Task 1 was completed successfully.

Results Task 2 – Campaign Performance

Task 2 focused on performance of the campaign – essentially to perform stationary and mobile measurements in and around Corpus Christi and San Antonio from April 1 until May 19, 2021. From April 1 through April 22, 2021, the On the Beach RV Park in Port Aransas outside Corpus Christi was used as the home base. Stationary measurements were conducted at this location from April 2 through the morning of April 15. From April 15 through the morning of April 22, this location served as the overnight location for sampling, but during the day, mobile sampling downwind of Corpus Christi was performed. On the morning of April 22, the home base was moved to Traveler's World RV Park near the core of urban San Antonio. From April 22 through April 29, this second RV park was used as the overnight location for sampling, but during the day, mobile sampling upwind of San Antonio was performed. This location was also used as the location for stationary sampling from April 29 until May 12. For the final week, Traveler's World was used as the home base at night while sampling occurred downwind of San Antonio in mobile mode during the day, including at the campus of the University of Texas at San Antonio, for comparison to SAFS data. Based on the successful collection of data across the multiple weeks of the project in all locations specified and the large percentage of data coverage, Task 2 was completed successfully.

Results Task 3 – Data Analysis, Field Campaign

For this report, only portions of time series or overview plots are shown for the sake of brevity. For example, Figure 4 indicates the time series of both inorganic trace gases and meteorological parameters during stationary sampling at the On the Beach RV Park in Port Aransas. Similar data are shown in Figure 5 for the Traveler's World RV Park near the urban core of San Antonio.

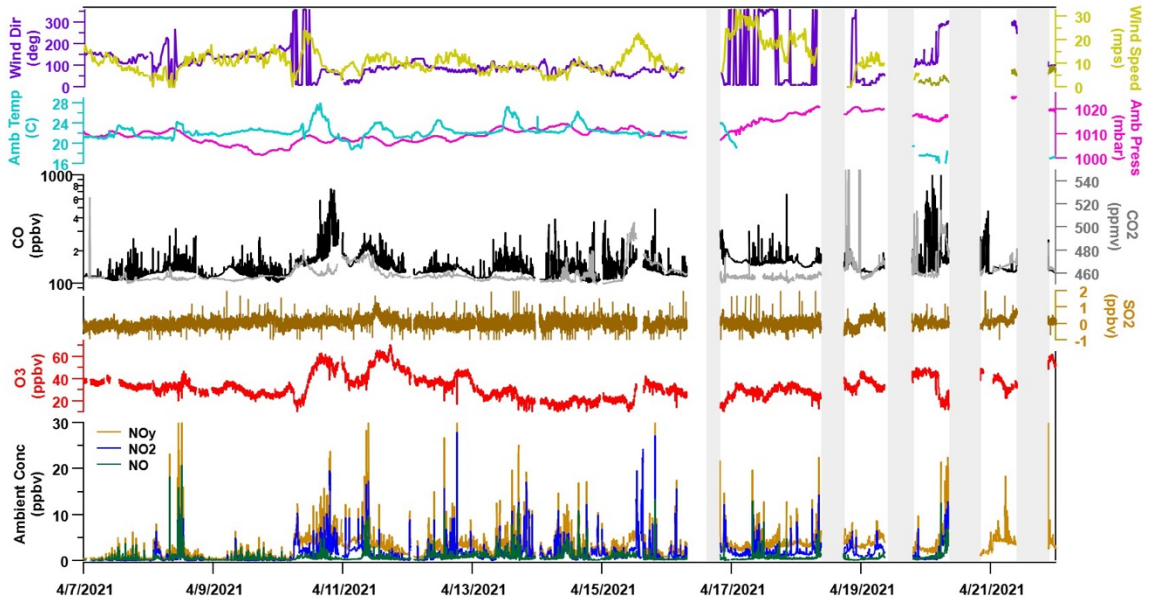

Figure 4. Corpus Christi, Port Aransas stationary time series of trace gas (1-minute averages) and meteorological (5-to-15-minute averages) measurements. The shaded gray areas in figure were during mobile periods. Trace gases include NO (ppbv, green), NO_2 (ppbv, blue), NO_y (ppbv, light orange), O_3 (ppbv, red), SO_2 (ppbv, dark orange), CO (ppbv, black), and CO_2 (ppmv, gray) data. Meteorological data include wind direction (degrees, purple), wind speed (mps, dark yellow), ambient temperature (degrees light green), and ambient pressure (mbar, pink).

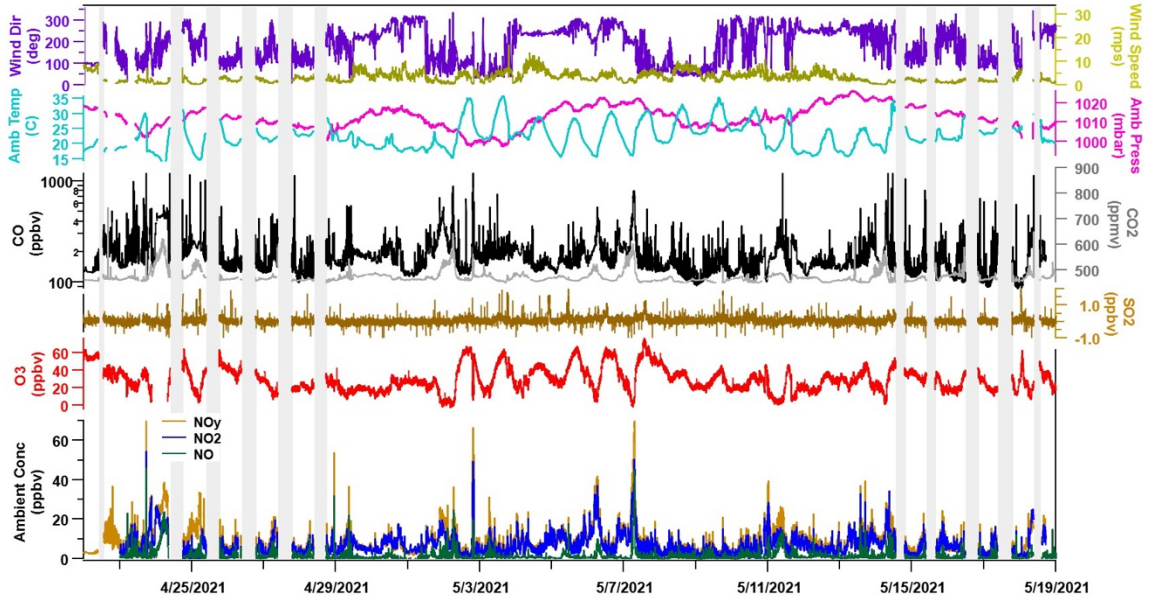

Figure 5. Traveler's World, San Antonio stationary time series of trace gas (1-minute averages) and meteorological (5-minute averages) measurements. The shaded gray areas in figure were during mobile periods. Trace gases include NO (ppbv, green), NO_2 (ppbv, blue), NO_y (ppbv, light orange), O_3 (ppbv, red), SO_2 (ppbv, dark orange), CO (ppbv, black), and CO_2 (ppmv, gray) data. Meteorological data include wind direction (degrees, purple), wind speed (mps, dark yellow), ambient temperature (degrees light green), and ambient pressure (mbar, pink).

During the stationary periods in Corpus Christi, average NO, NO_2, and NO_y concentrations were 0.63 ± 0.84 ppbv, 1.45 ± 1.97 ppbv, and 8.36 ± 0.84 ppbv, respectively. Average O_3, CO, SO_2, and CO_2 concentrations were 32.5 ± 10.7 ppbv, 146 ± 53 ppbv, 0.05 ± 0.30 ppbv, and 460 ± 12 ppmv, respectively. During stationary periods at Traveler's World (San Antonio) NO, NO_2, and NO_y concentrations were 1.17 ± 2.49 ppbv, 6.28 ± 5.08 ppbv, and 6.52 ± 4.54 ppbv, respectively. Average O_3, CO, SO_2, and CO_2 concentrations were 29.3 ± 13.5 ppbv, 178 ± 84 ppbv, 0.06 ± 0.20 ppbv, and 472 ± 22 ppmv, respectively. In general, higher mixing ratios and more variability in pollutant levels were observed in the stationary San Antonio dataset. Overall, larger contribution of NO_2 and NO relative to NO_y in San Antonio is indicative of fresher, less aged emissions. More detailed analysis will be performed in the future.

The type of event that will undergo further analysis is a bay breeze/sea breeze event that occurred the morning of April 20. During this period, meteorological data showed wind shifts and changes in temperature and relative humidity followed by increased pollution concentrations (Figures 6 and 7). Early morning winds, at approximately 3:00 CST, were from the southeastern direction (marine) followed by shifts to the northwestern direction (continental). During this period, the boundary layer height also was consistently less than 1 km (Figure 8). Increased levels of aerosol and trace gases were observed during the period (Figure 6 and 7). To confirm that the instruments were not sampling local emissions from the RV park, at approximately 08:20 CST, the MAQL2 was moved to a vacant parking lot more upwind of local anthropogenic emissions. At this secondary site, elevated pollution concentrations also were observed.

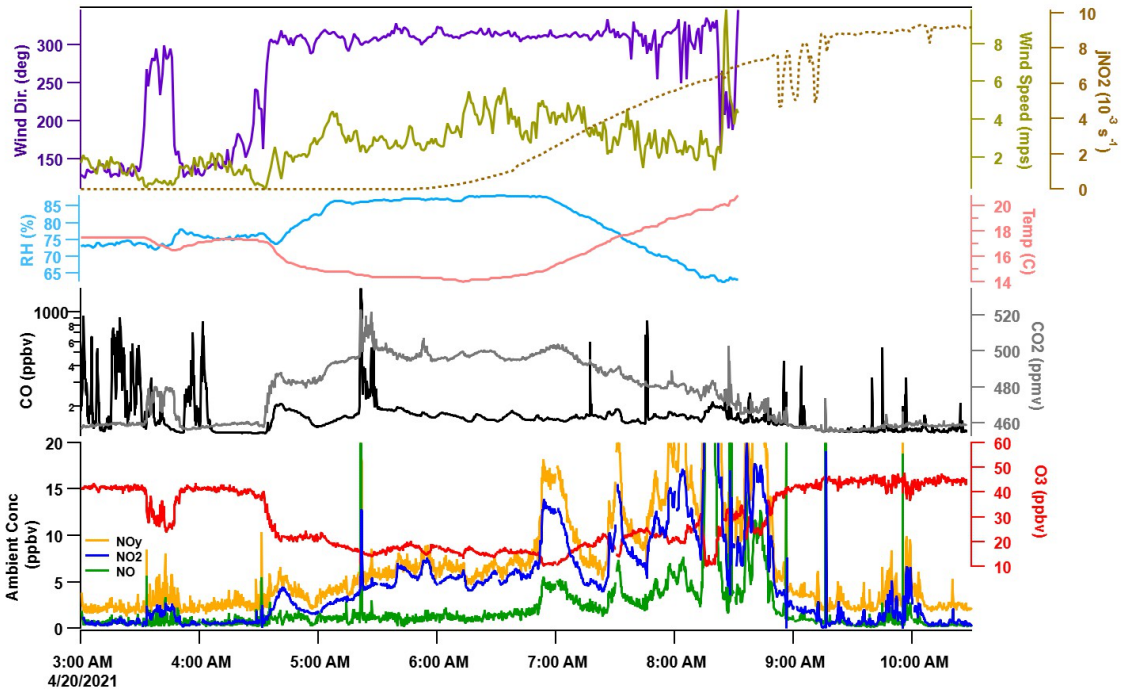

Figure 6. Trace gas (10-second) and meteorological (1-minute) measurements during the bay breeze event on April 20, 2021. Trace gases include NO (ppbv, green), NO_2 (ppbv, blue), NO_y (ppbv, light orange), O_3 (ppbv, red), SO_2 (ppbv, dark orange), CO (ppbv, black), and CO_2 (ppmv, gray) data. Meteorological data include wind direction (degrees, purple), wind speed (mps, dark yellow), ambient temperature (degrees light green), and ambient pressure (mbar, pink). The photolysis rate of NO_2, j_{NO2} (10^{-3} s^{-1}, dark yellow) is also included in the figure.

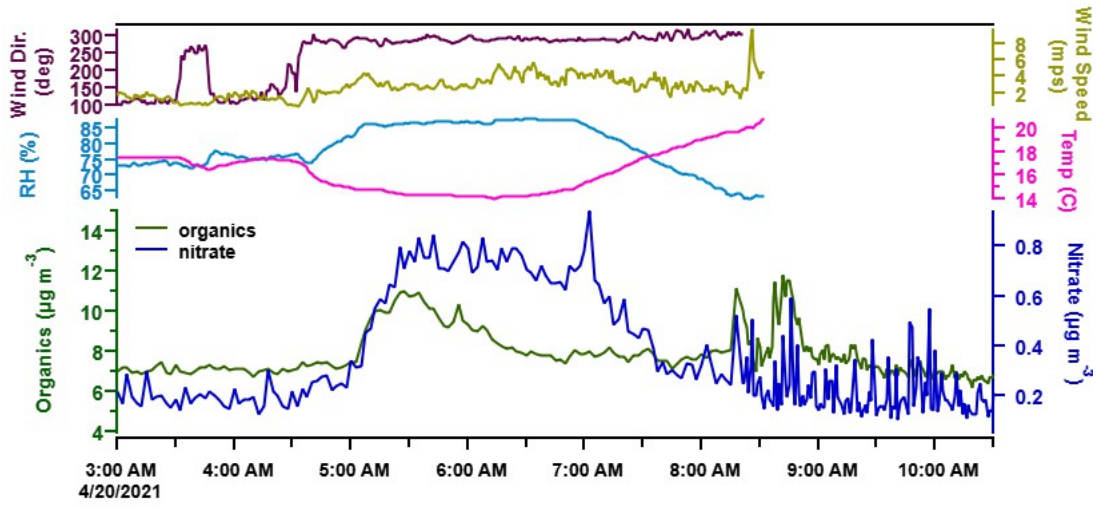

Figure 7. Aerosol (2 to 3-minute) and meteorological (1-minute) measurements during the bay breeze event on April 20, 2021. Representative aerosol measurements include bulk organic (µg m^{-3}, green) and bulk nitrate (µg m^{-3}, blue) measurements. Meteorological data include wind direction (degrees, purple), wind speed (mps, dark yellow), ambient temperature (degrees light green), and ambient pressure (mbar, pink).

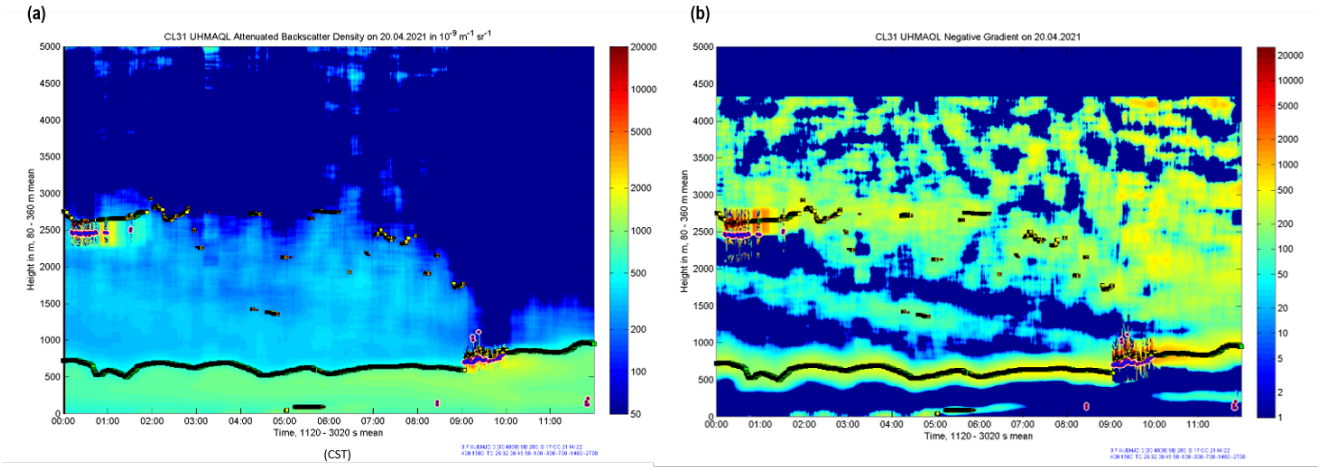

Figure 8. Boundary layer height (m) from the CIMEL Lidar data on the morning of April 20, 2021 which includes (a) attenuated backscatter density ($10^{-9}m^{-1}s^{-1}$) and (b) negative gradient data.

The following figures indicate various VOC time series. Figure 9 indicates stationary measurements in Corpus Christi of benzene, toluene, xylene, isoprene, monoterpenes, MVK+MACR, and MEK, while Figure 10 indicates stationary and mobile measurements of oxygenated VOCs (acetaldehyde and acetonitrile), acetone, and DMS and styrene, also in Corpus Christi. Significant variability is observed in every time series, regardless of sampling mode.

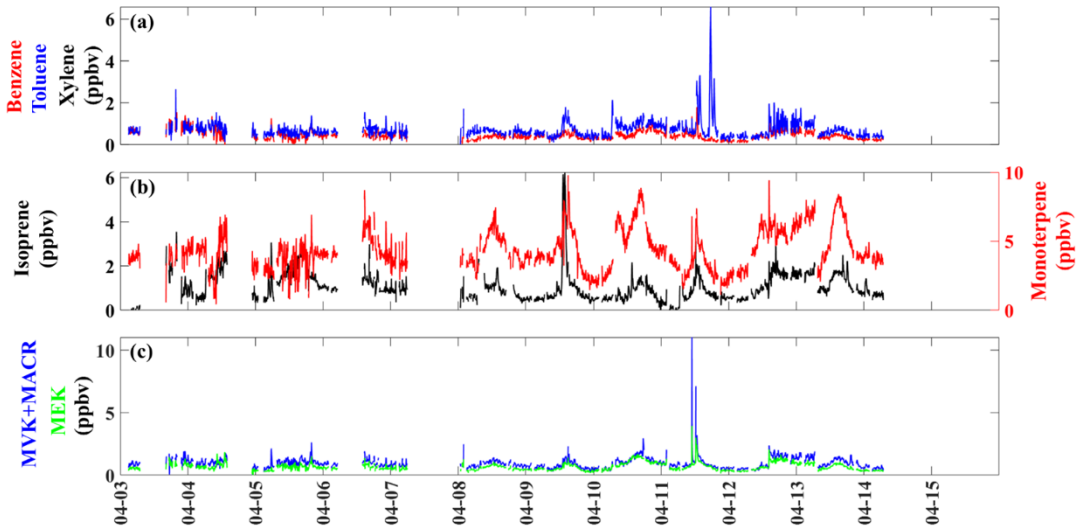

Figure 9. Corpus Christi, Port Aransas stationary time series (5-minute average, ppbv) of **(a)**, anthropogenic VOCs (benzene, toluene and xylene), **(b)** biogenic VOCs (isoprene and monoterpene), and **(c)** secondary VOCs (MVK+MACR, MEK).

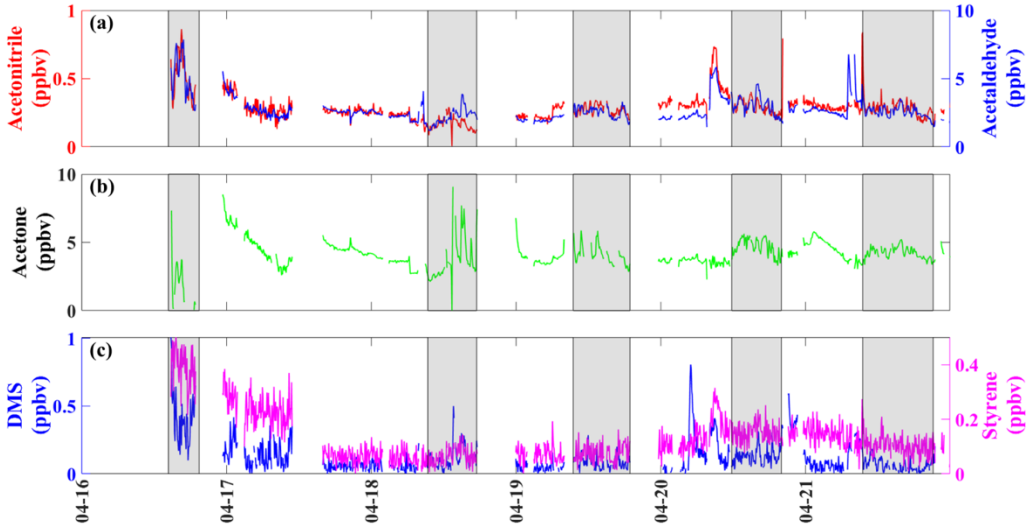

Figure 10**.** Corpus Christi, Port Aransas time series (5-minute average, ppbv) of **(a)** oxygenated VOCs (acetaldehyde and acetonitrile), **(b)** acetone, and **(c)** DMS and styrene. Mobile measurement time periods are designated by grey color shaded boxes.

Conversely, Figure 11 shows the stationary time series of HCHO at the Traveler's World location in San Antonio. Of all VOC time series shown in this report, HCHO in stationary mode near San Antonio shows not only the largest magnitude of mixing ratio (approaching 20 ppbv) but also the most regular diurnal pattern.

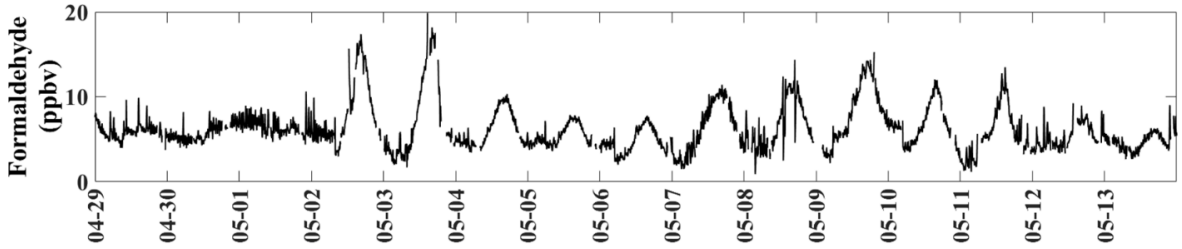

Figure 11. Traveler's World, San Antonio stationary time series (5-minute average, ppbv) of HCHO.

An overview of all HR-ToF-AMS data across the entire campaign including both stationary and mobile measurements in both cities is provided in Figure 12. The background shading indicates location and mode of sampling. Meteorological data and some trace gases also are provided for reference. The time series of non-refractory submicron aerosol (NR-PM_1) loading and its major five constituents (4th panel from the top) show considerable variability. NR-PM_1 during the entire sampling period averaged 14.4 ± 8.5 μg m^{-3}. Large spikes and concentrations that approach almost 100 μg m^{-3} were observed, which were associated with primary PM emissions from combustion sources, although more typical concentrations are approximately 10-15 μg m^{-3}.

The fifth panel shows the time-dependent aerosol composition. On campaign average, organics dominated the composition, making up 45% of the total mass, following by sulfate (38%), ammonium (13%), nitrate (3%), and chloride (1%). For the first two weeks at Port Aransas, sulfate contributed more than half of the total aerosol mass under the influence of marine airmasses, as indicated by southerly wind (1st panel), and episodic high chloride reached up to 3 μg m^{-3}. The sixth panel shows oxygen-to-carbon (O/C) ratio and hydrogen-to-carbon (H/C) ratio of organic aerosol and the fraction of the signal at m/z 60 in the organic aerosol spectrum (f_{60}). The variability of these three parameters indicates the importance of various types of organic aerosol and emphasize the importance of performing PMF on this data set. Higher values of O/C indicate aged/processed particles, while higher values of H/C indicate the importance of primary emissions of organic aerosol. Increased values of f_{60} show the influence of biomass burning. The O/C generally showed decreasing trend as moving from Port Aransas by the coast to inland San Antonio, suggesting less oxidized and processed particles in San Antonio area. The H/C was much higher during the mobile measurements than the adjacent stationary measurements, emphasizing greater contribution from traffic emissions on road. Transported wildfire plumes with elevated CO mixing ratio, organic mass concentration, and f_{60} well above 0.3%, the threshold value for biomass burning influenced aerosols, were observed April 10 – April 12.

The bottom two panels show the time series of seven OA factors derived from PMF analysis and their mass fractional contribution to total OA. Each OA factor has distinct temporal variation and mass spectral features and are associated with different sources and processes. To perform PMF, the spectral matrices of organic and inorganic species were combined, and the ion signals were expressed in nitrate-equivalent concentrations. The HR-MS of organic ions for m/z 12 – 180 were included. For inorganics, only the major ions for each species were included (SO^+, SO_2^+, HSO_2^+, SO_3^+, HSO_3^+, and $H_2SO_4^+$ for sulfate; NO^+ and NO_2^+ for nitrate; NH^+, NH_2^+, and NH_3^+ for ammonium; and Cl^+ and HCl^+ for chloride). After PMF analysis, the mass concentration of each factor was derived from the sum of organic signals in the corresponding

mass spectrum after applying the RIE (=1.4) for organics and the CE described previously. The solutions for 2 to 9 factors were explored at a fixed rotational parameter. After a detailed evaluation of mass spectral profiles, temporal trends, diurnal variations, and correlations with ions, the seven-factor solution was chosen. These seven factors are: 1) hydrocarbon-like organic aerosol (HOA) that is associated with traffic-related primary emissions (contributing on average 10% of total organic aerosol mass), 2) biomass burning organic aerosol (BBOA; 12%) associated with campfires as well as regional transported wildfire plumes, 3) less-oxidized oxygenated organic aerosol (LO-OOA) representing less processed and fresher SOA (O/C = 0.51; 30%), 4) more-oxidized OOA (MO-OOA) possibly representing more processed and aged SOA (O/C = 1.22; 30%), 5) an OOA that was associated with ammonium nitrate and biomass burning (AN-BB-OOA; 3%), 6) a highly oxidized OOA associated with ammonium sulfate (AS-OOA; 13%), and 7) a highly oxidized OOA associated with acidic sulfate (acidic-OOA; 3%). The time series, mass spectra and diurnal profiles of each of these factors are shown in Figure 13. The importance of these factors varies strongly with time and space.

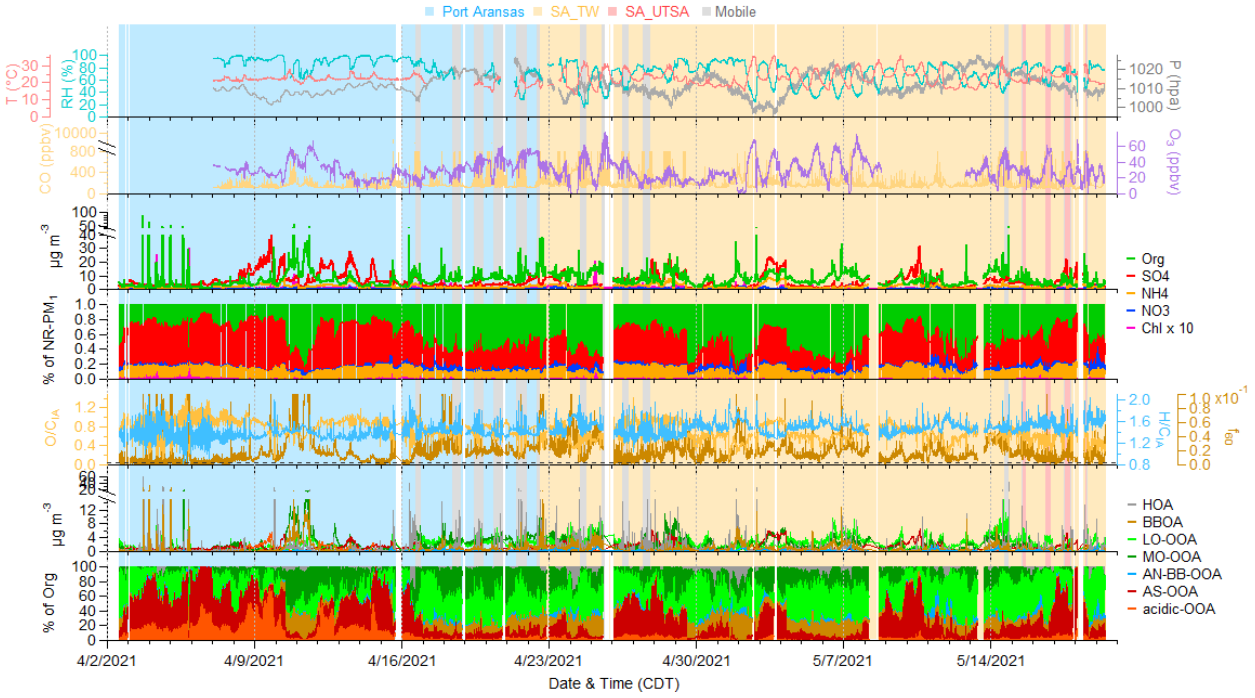

Figure 12. Time series of temperature (T), relative humidity (RH), and pressure (P); CO and O_3 mixing ratio (ppbv); aerosol composition (μg m^{-3}) and fractional composition; oxygen-to-carbon (O/C) ratio and hydrogen-to-carbon (H/C) ratio of organic aerosol and the fraction of the signal at m/z 60 in the organic aerosol spectrum; and PMF-determined concentrations (μg m^{-3}) and fractional composition. Colored shades indicate periods of stationary sampling at three locations: On the Beach RV Park in Port Aransas, Travelers World RV Park in San Antonio (SA_TW), and the University of Texas at San Antonio (SA_UTSA), respectively. Gray shades indicate periods of mobile sampling.

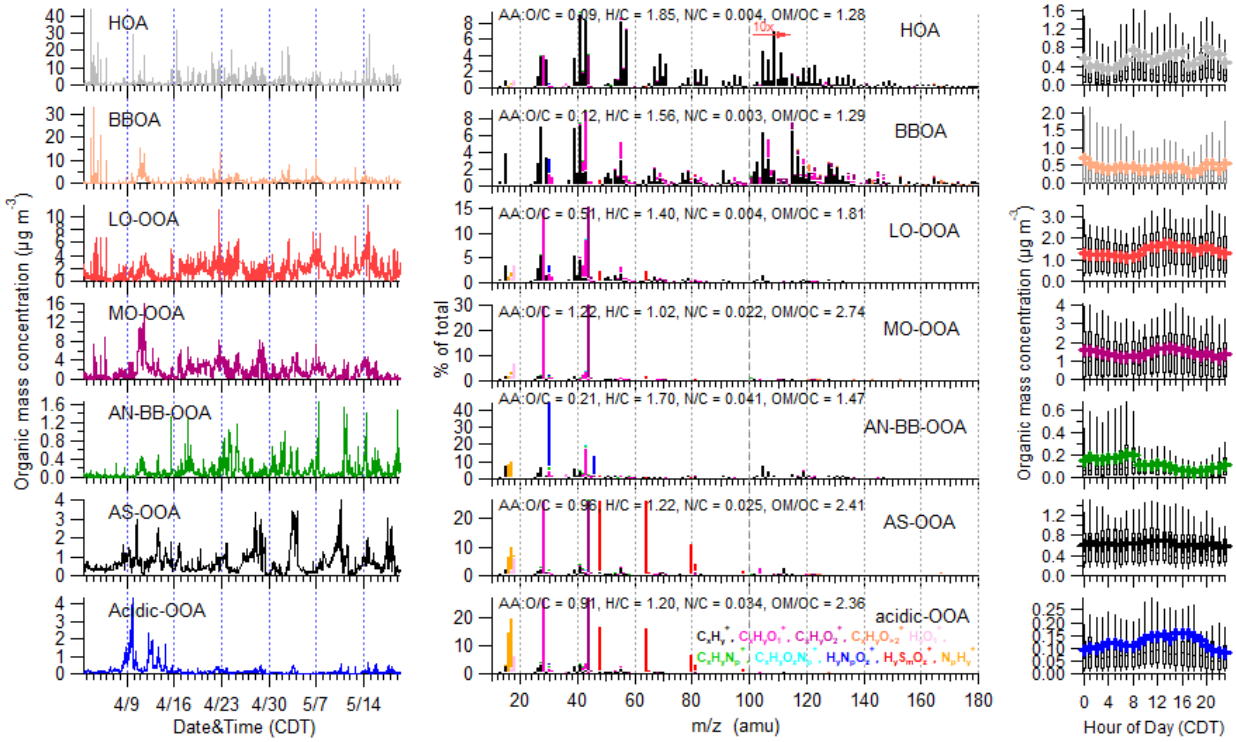

Figure 13. (left) Time series of seven organic aerosol factors; (middle) high-resolution mass spectra of organic aerosol factors and their associated inorganic ions colored by ten ion families. The elemental ratios of each factor are shown in each panel; (right) Diurnal profiles of organic aerosol factors. The whiskers above and below the boxes indicate the 90th and 10th percentiles, the upper and lower boundaries, respectively, indicate the 75th and 25th percentiles, the lines in the boxes indicate the median values, and the cross symbols indicate the mean values.

Figure 14 compares stationary measurements of NR-PM_1 made in Port Aransas (PA) and two locations in San Antonio (Traveler's World (TW) and UT-San Antonio). Because only limited measurements were conducted at the second San Antonio site, those results will not be discussed further in this report. The pie charts on the top of the figure show total composition on the left; while average concentrations were larger at TW, on a fractional basis the importance of sulfate decreased and that of OA increased moving inland. The pie charts on the right show composition of OA based on the PMF results. Here, the biggest differences are the increase in the fresher SOA LO-OOA and the decrease in the acidic-OOA moving from PA to TW.

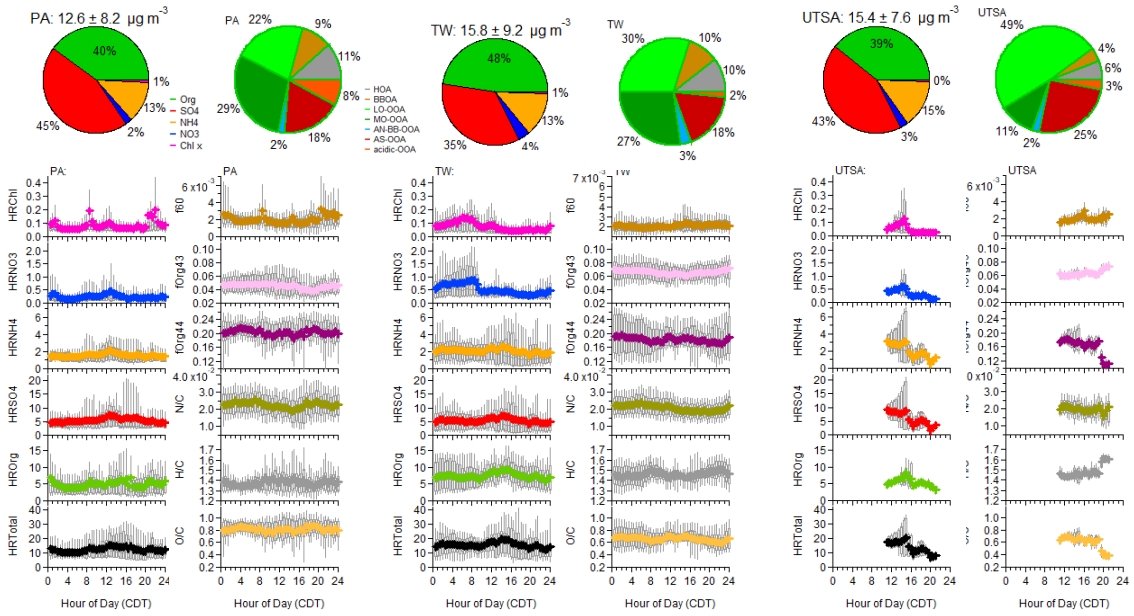

Figure 14. Diurnal variations and fractional contributions of species mass concentrations and the chemical properties and elemental ratios of organic aerosol for stationary measurements at three locations: On the Beach RV Park in Port Aransas (PA), Travelers World RV Park in San Antonio (TW), and the University of Texas at San Antonio (UTSA), respectively. The whiskers above and below the boxes indicate the 90th and 10th percentiles, the upper and lower boundaries of boxes, respectively, indicate the 75th and 25th percentiles, the lines in the boxes indicate the median values, and the colored cross symbols indicate the mean values.

As with the trace gas and VOC time series shown previously, only a portion of the aerosol optical property time series are shown here. Figure 15 indicates stationary/mobile measurements of σ_{abs} (Mm^{-1}) in Corpus Christi for three wavelengths and the calculated AAE based on these measurements. A large spike (approaching 100 Mm^{-1}) in σ_{abs} can be observed prior to the first mobile measurement period (the gray shade). The stationary measurements of σ_{scat} (Mm^{-1}) shown in Figure 16 show much greater variability, a larger magnitude, and more consistent diurnal behavior (opposite of that of the calculated SAE that also is shown). The SSA shown for San Antonio during stationary measurements in Figure 17 shows periods where this calculated parameter approaches unity (purely scattering aerosol); however, periods of SSA less than 0.5 indicate significant contribution of light absorption to total extinction caused by PM.

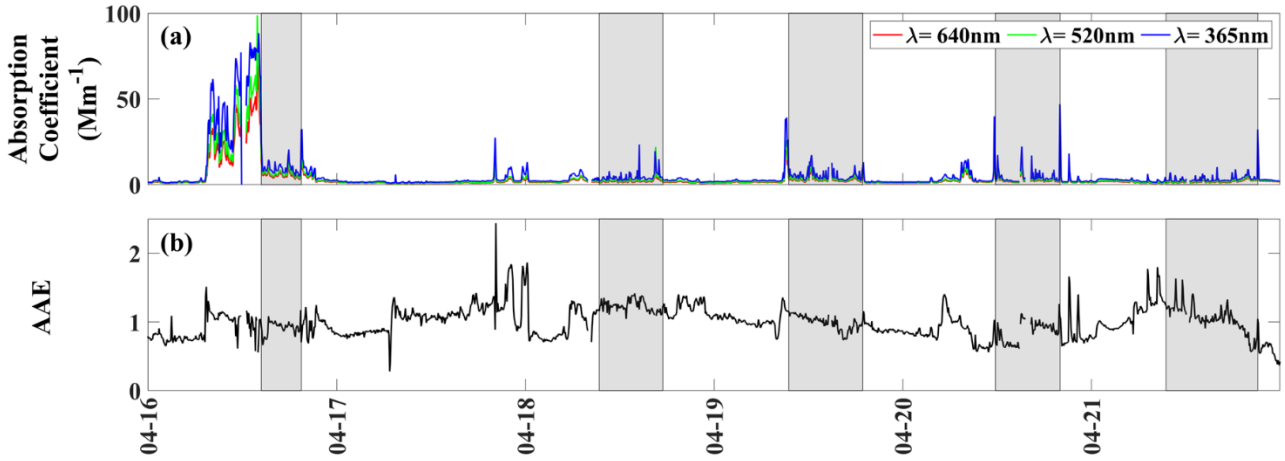

Figure 15. Corpus Christi, Port Aransas time series (5-minute average) of **(a)** σ_{abs} (Mm^{-1}) at three different wavelengths (640 nm, 520 nm and 365 nm) and **(b)** AAE. Mobile measurement time periods are designated by grey color shaded boxes.

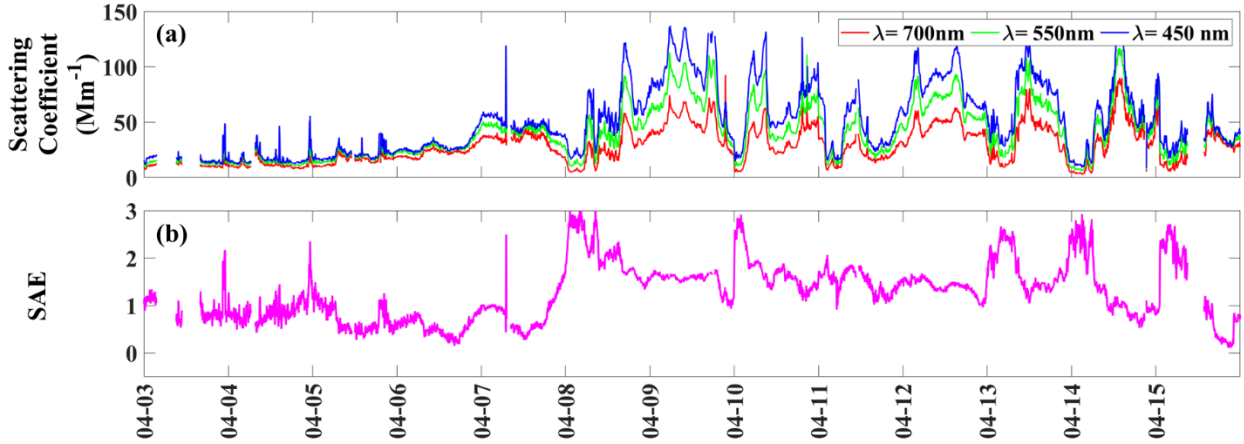

Figure 16. Corpus Christi, Port Aransas stationary time series (5-minute average) of (a) σ_{scat} (Mm^{-1}) at three different wavelengths (700 nm, 550 nm and 450 nm) and (b) SAE.

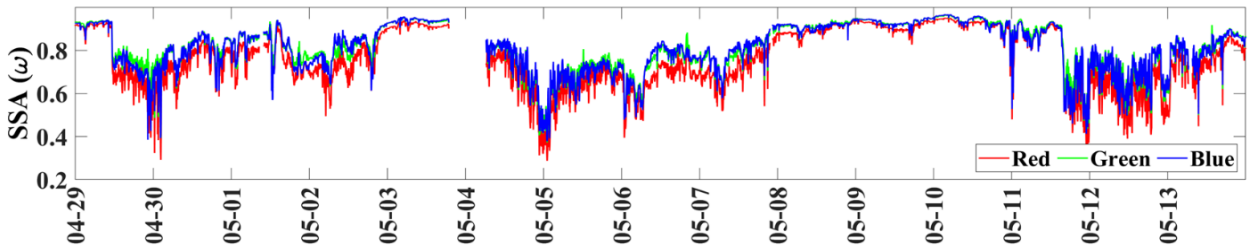

Figure 17. Traveler's World, San Antonio stationary time series (5-minute average) of SSA.

Results Task 3 – Data Analysis, Modeling

The first task associated with the 3D air quality modeling efforts is the comparison of model output to observed data using publicly available information. This includes hourly O_3 mixing ratios and meteorological variables including wind speed and direction, air temperature, and relative humidity from continuous ambient monitoring stations (CAMS) maintained by the TCEQ. Afternoon mean was defined as 1:00 pm to 6:00 pm CDT and was chosen as the appropriate time metric, as it is the common period across all domains at various output frequencies. Second, the choice of daytime mean O_3 circumvents the known problem of overestimating nighttime O_3 common to all global models. Data from the TROPOspheric Monitoring Instrument (TROPOMI), launched in October 2017, also were utilized. In this study, the offline TROPOMI NO_2 retrieval (version 1.4) of April and May 2021 was used. A physical oversampling approach was applied to TROPOMI NO_2 column retrievals. For quality assurance, only observations with overall quality flag (qa_value) greater than 0.75 and retrieved cloud fraction (cloud_fraction) less than 0.3 are used. To properly compare TROPOMI NO_2 retrievals with simulated WRF-GC NO_2, TROPOMI averaging kernels were applied to WRF-GC NO_2 using documented procedures.

The GEOS-Chem global chemical transport model has a standard benchmarking procedure for each major code release, using observations compiled from surface monitoring network, aircraft campaigns, and satellite retrievals around the globe. In addition to these efforts, an in-depth evaluation of the model's performance in simulating field observations was performed. Table 4 shows the performance metrics employed throughout the reporting periods for this study. In addition to the performance metrics, descriptive statistics such as mean, median, standard deviation, minimum, and maximum were computed for all boundary conditions produced.

Table 4. Performance metrics of the GEOS-Chem model.

Correlation Coefficient (R)	$R = \frac{\sum_{i=1}^{N}(M_i - \overline{M})(O_i - \overline{O})}{\sqrt{\sum_{i=1}^{N}(M_i - \overline{M})^2}\sqrt{\sum_{i=1}^{N}(O_i - \overline{O})^2}}$
Normalized Mean Bias (NMB)	$NMB = \frac{\sum_{i=1}^{N}(M_i - O_i)}{\sum_{i=1}^{N} O_i} \times 100\%$
Root Mean Square Error (RMSE)	$RMSE = \sqrt{1/N\sum_{i=1}^{N}(M_i - O_i)^2}$

Note: M is the model output, O is the observation, N is the number of samples, and $\overline{M} = 1/N\sum_{i=1}^{N} M_i$, $\overline{O} = 1/N\sum_{i=1}^{N} O_i$.

This section shows spatial and temporal variations of O_3, CO, and meteorological variables including ambient temperature and relative humidity. Spatial variations are evaluated using 12-day mobile tracks of 21–22 April, 24–28 April, and 14–18 May, 2021. Temporal variations are evaluated using 10-day stationary observations of 7–15, and 17 April at On the Beach, and 12-

day stationary observations of 23 April, 29–30 April, 1–8 May, and 13 May, 2021, at Traveler's World.

Figure 18 compares the spatial pattern of O_3, CO, temperature and relative humidity for 21–22 April, 24–28 April, and 14–18 May, 2021, between campaign field observations and the WRF-GC simulations. Table 5 provides detailed statistics for the comparisons, which indicates that modeled meteorological variables are in good agreement with observed values, while air pollutants show lesser agreement. Modeled mean temperature of 23.25 ± 4.05 °C is consistent with observed value of 22.55 ± 3.95 °C (R = 0.76; RMSE=2.84 °C). Modeled mean relative humidity of 70.45 ± 20.40 % matches the observed value of 69.44% ± 16.84 % (R = 0.74; RMSE = 13.79%).

The model sees an overestimation of mean O_3 concentration of 49.10 ± 13.65 ppbv in comparison to an observed value of 31.35 ± 13.58 ppbv. The model has concentrations 56% higher than observations, with R = 0.71 and RMSE = 20.56 ppbv. This overestimation is likely due to an overestimation of regional background O_3 because this high bias is persistent along the mobile tracks over the rural region (29°–29.5°N and 97°–98°W; northeast track), as shown in Figure 18. After removing mean biases of 20 ppbv, the corrected model concentrations of 29.10 ± 13.65 ppbv fall within a similar level as the observed values of 31.35 ± 13.58 ppbv in Figure 19. The corrected model shows better agreement with concentrations 7% lower than observations and RMSE=10.63 ppbv.

The model sees an underestimation of mean CO concentration of 127.88 ± 18.42 ppbv in comparison to an observed value of 183.32 ± 160.46 ppbv. High CO measurements above 150 ppbv were observed along the highway IH-37 from Corpus Christi to San Antonio and in the urban center of San Antonio, both of which the model does not capture in Figure 18. It is likely that highway and urban emissions are underestimated in the model. Figure 20 shows the density distribution of observed versus modeled CO, where a long tail of observed CO goes toward higher than 150 ppbv. To validate background CO, a test is conducted by removing both observed and modeled grids where observed CO is above 150 ppbv (Figure 19). After removing the high concentration data points, CO correlation improves from 0.24 to 0.41, NMB from –30% to –5%, and RMSE from 166.48 to 16.81 ppbv.

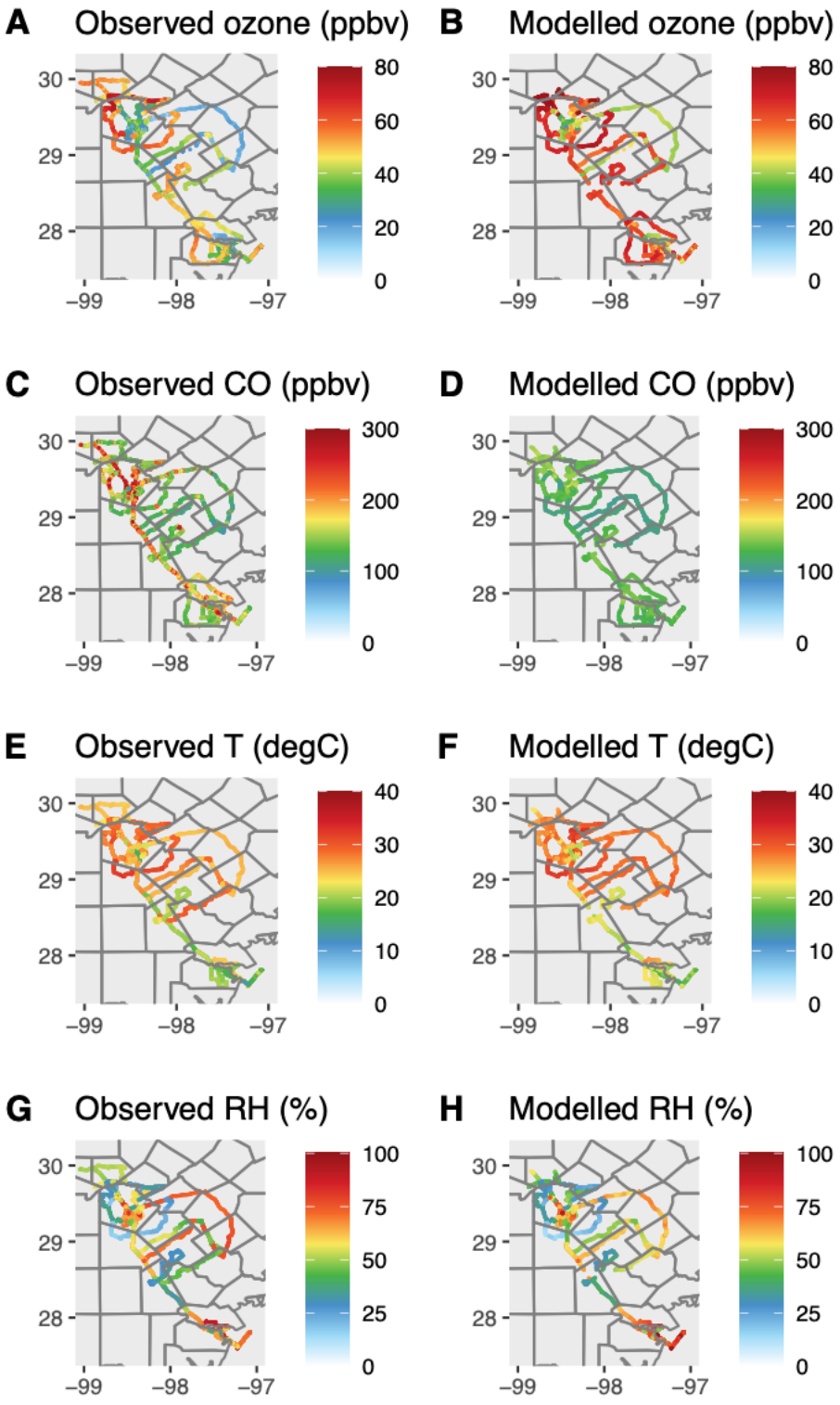

Figure 18. Observed (left panel) and modeled (right panel) O_3, CO, temperature, and relative humidity at the mobile sampling tracks during the field campaign. Mobile tracks shown are the combinations of measurements during 21–22 April, 24–28 April, and 14–18 May, 2021.

Table 5. Performance metrics of the WRF-GC simulations (1 km x 1 km resolution) in comparison with mobile observations of the field campaign. All units are inserted, unless stated otherwise. * denotes supplementary performance metrics for O_3 and CO. *Ozone_Background20 is a correction of modeled regional background high O_3 by deducting a mean bias of 20 ppbv. *CO_NoHighway is removing observed high CO concentrations above 150 ppbv along the highway IH-37.

	OBS	MOD	R	NMB	RMSE
Ozone	31.35 ppbv	49.10 ppbv	0.71	0.56	20.56 ppbv
*Ozone_Background20	31.35 ppbv	29.10 ppbv	0.71	–0.07	10.63 ppbv
CO	183.32 ppbv	127.88 ppbv	0.24	–0.30	166.48 ppbv
*CO_NoHighway	127.47 ppbv	121.36 ppbv	0.41	–0.05	16.81 ppbv
Temperature	22.55 °C	23.25 °C	0.76	0.03	2.84 °C
RH	69.44%	70.45%	0.74	0.01	13.79%

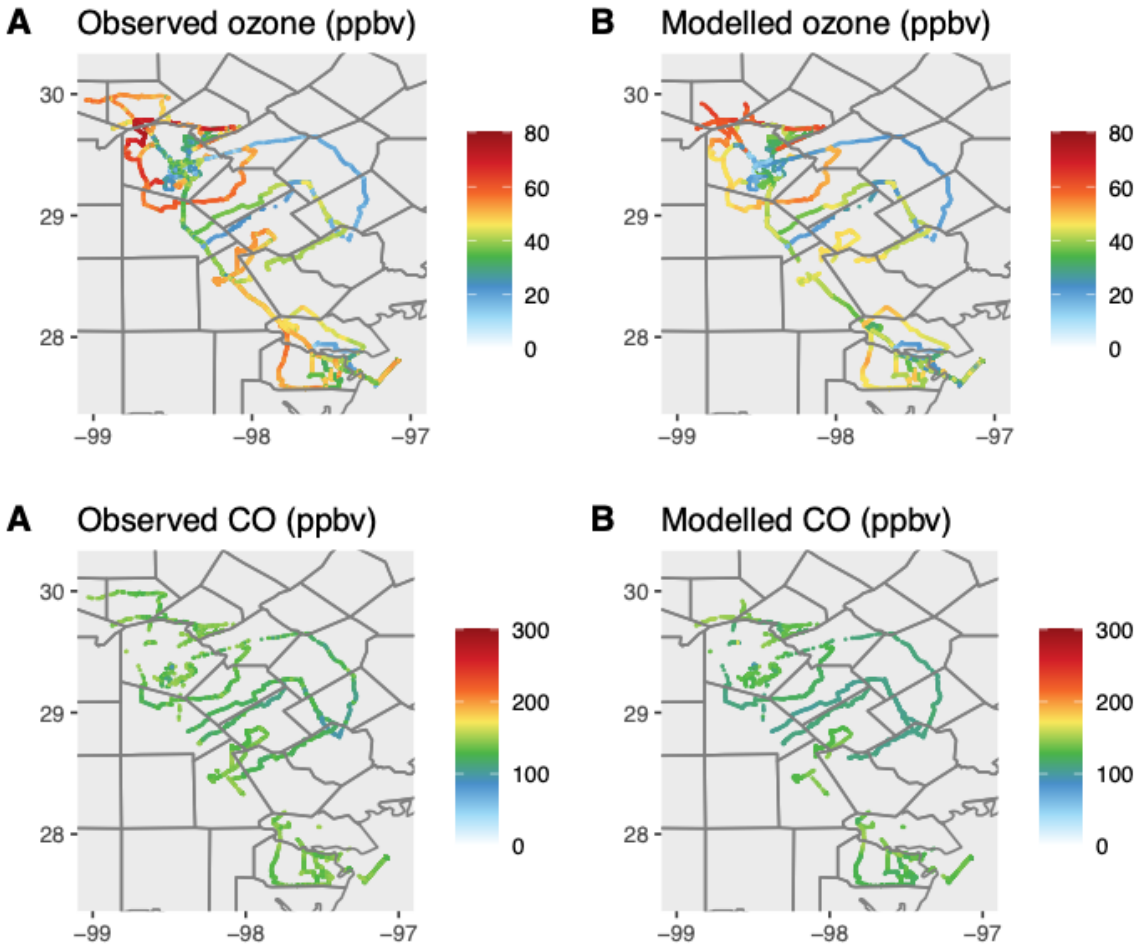

Figure 19. Same as O_3 and CO comparison in Figure 18 but for simulation Ozone_Background20 and CO_NoHighway in Table 5.

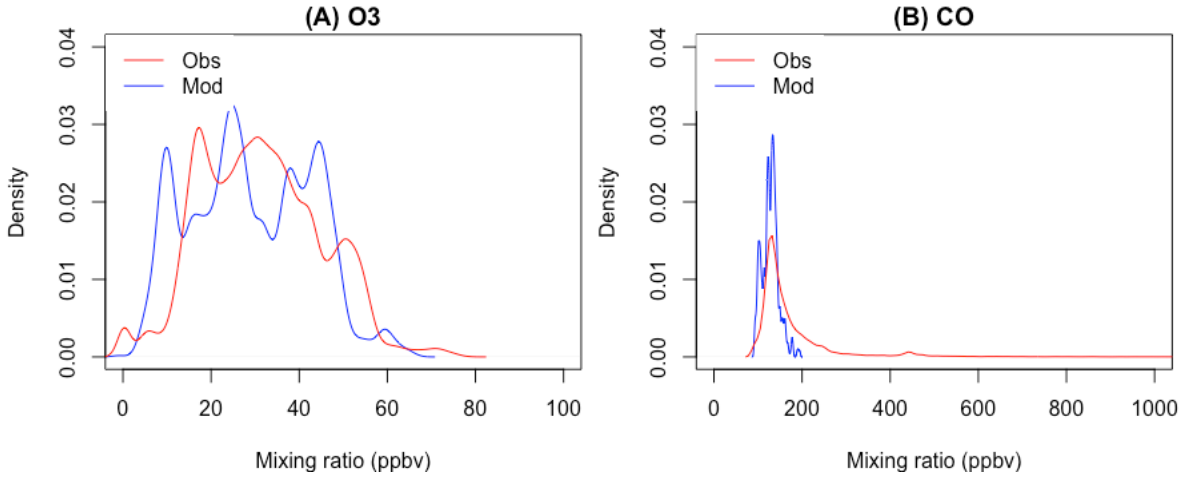

Figure 20. Density distribution of observed and modeled (a) O_3 and (b) CO.

Figure 21 and Figure 22 show the model reproduced diurnal and day-to-day variations well in comparison with two stationary sites, except for CO at Traveler's World, which may be due to local emissions causing the two spikes. Model performance of day-to-day variations in comparison with the field campaign is similar in magnitude as a comparison with TCEQ CAMS observations. The two high O_3 events, 11 April at On the Beach and 7 May at Traveler's World, are also captured by TCEQ CAMS observations in Figure 23. The two days experienced anticyclonic flow with warm and dry air over eastern Texas, which favored high O_3. Particularly O_3 peaked when maximum anticyclonic curvature of wind flow, i.e. the ridge line, was along the coast on both 11 April and 7 May, shown in Figure 24.

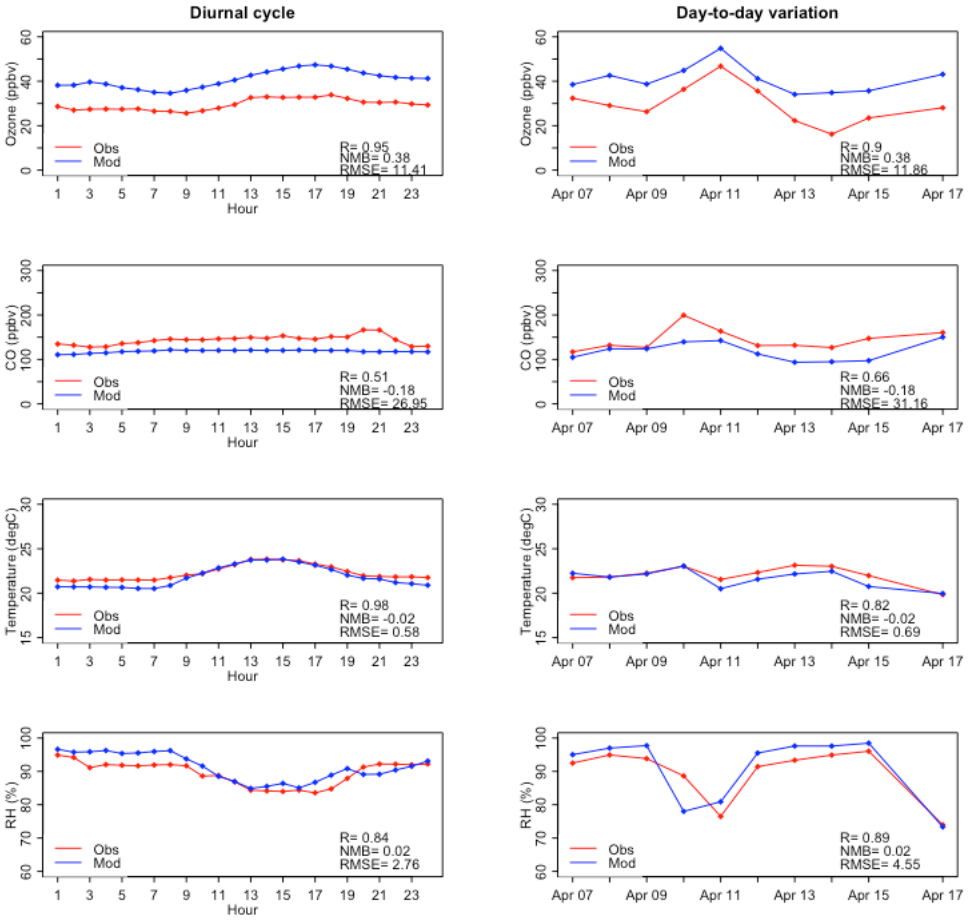

Figure 21. Observed and modeled O_3, CO, temperature, and relative humidity for 7–15 April and 17 April 2021 at On the Beach during the field campaign. Right and left panels show diurnal and day-to-day variations respectively.

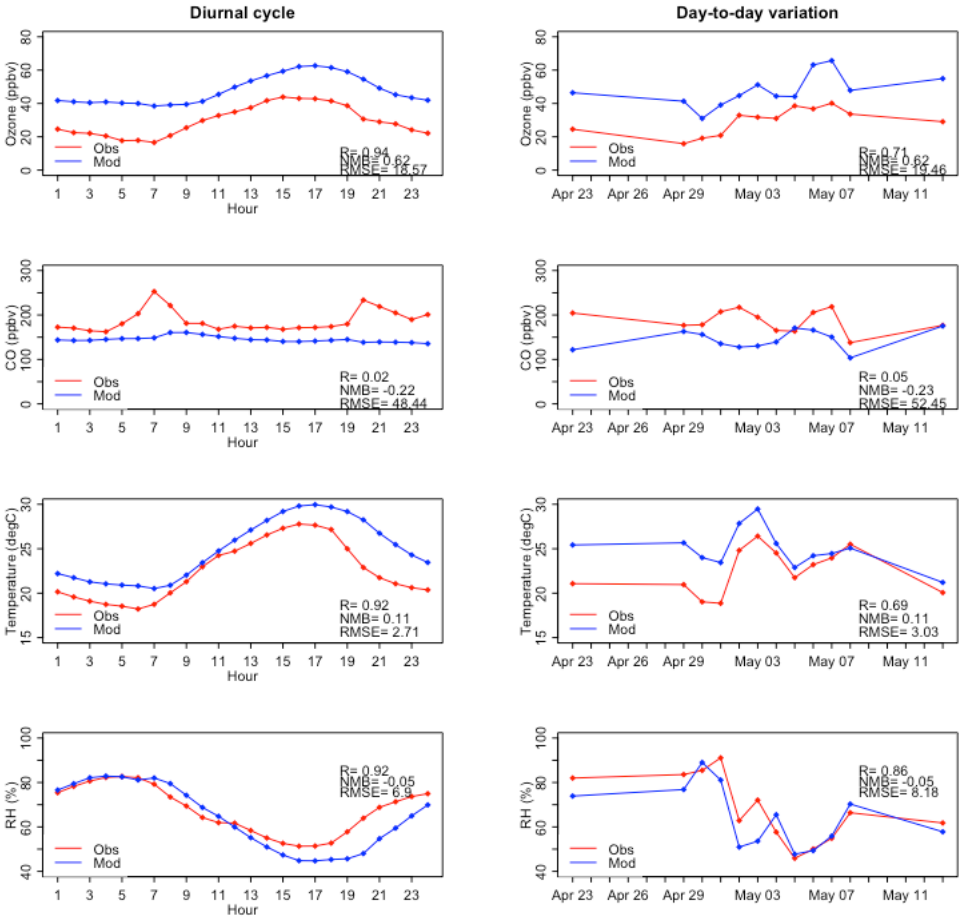

Figure 22. Observed and modeled O_3, CO, temperature, and relative humidity of 23 April, 29–30 April, 1–8 May, and 13 May 2021 at Traveler's World during the field campaign. Right and left panels show diurnal and day-to-day variations respectively.

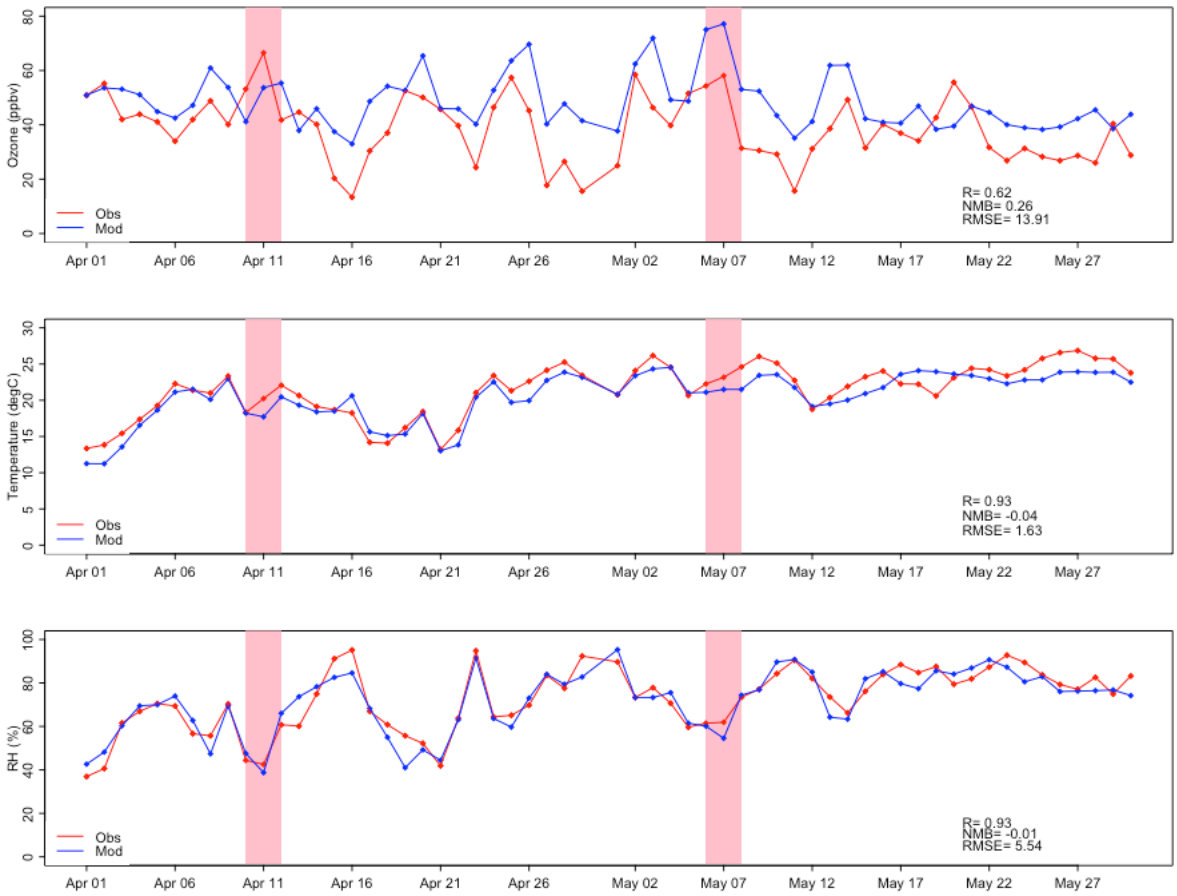

Figure 23. Ozone (upper), temperature (middle), and relative humidity (lower) observed by TCEQ CAMS and modeled by WRF-GC from 1 April to 30 May 2021. Pink shading denotes O_3 peaks observed at stationary sites during the campaign.

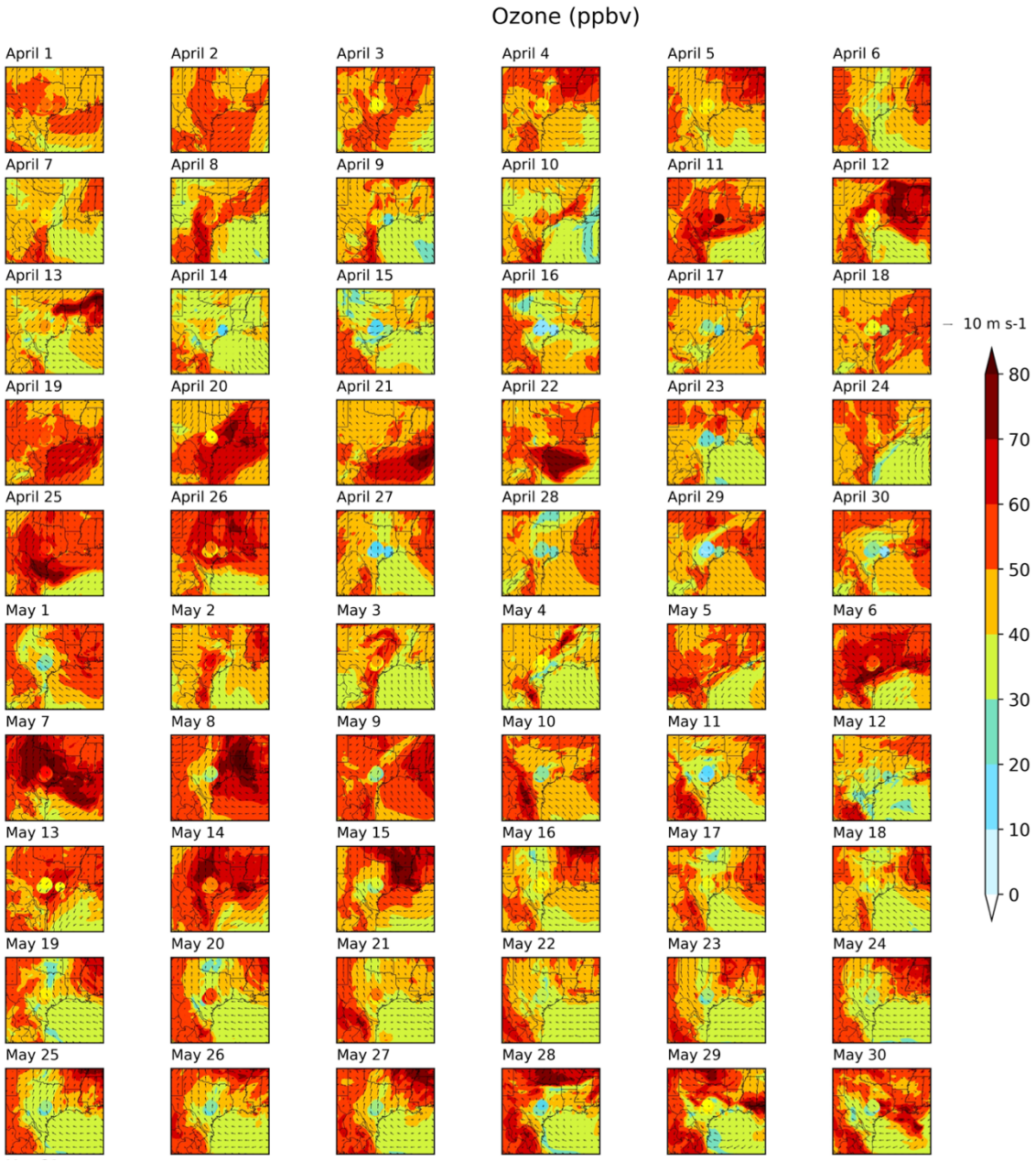

Figure 24. Daily afternoon mean O_3 concentrations from 1 April to 30 May 2021 of the WRF-GC simulations, overlaid with TCEQ CAMS observations (filled circles).

The model sees an underestimation of NO_2 vertical column densities in comparison with TROPOMI retrievals, particularly in urban areas (Figure 25). It is likely that the model does not capture urban NO_x emissions, similar to the finding with CO mentioned above. As both CO and NO_x are underestimated by the model, the strength of sources that emit both pollutions likely are underestimated, possibly both transportation and industry.

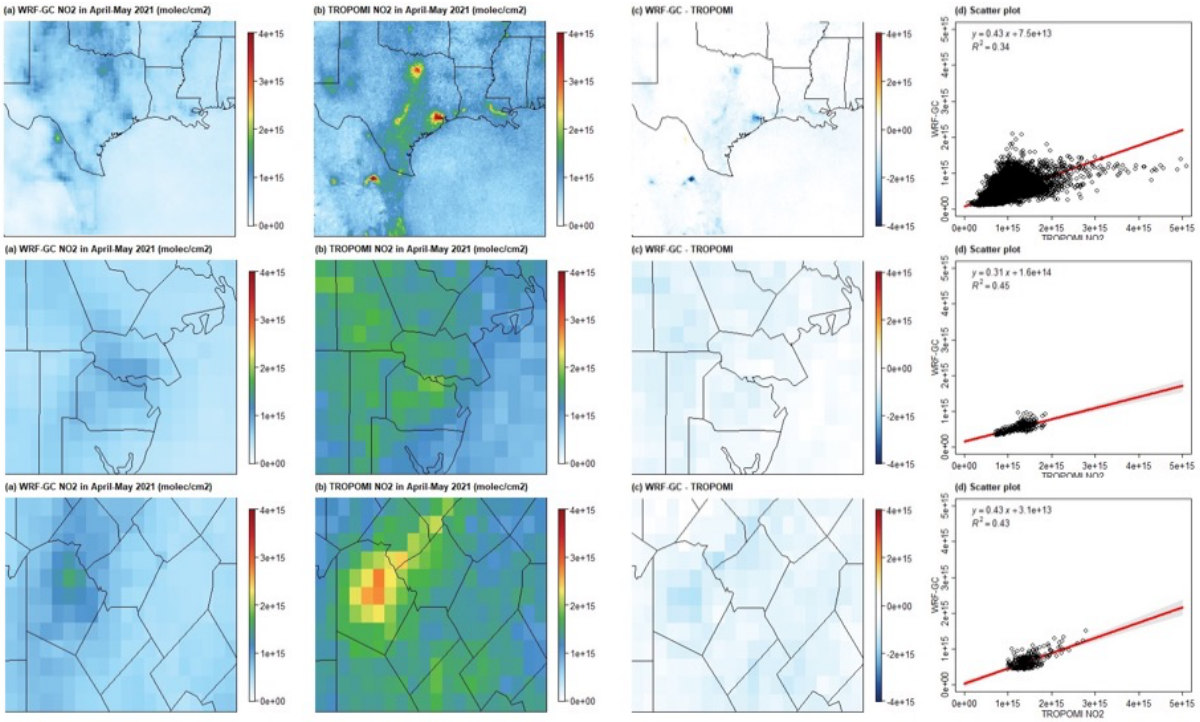

Figure 25. WRF-GC (a) and TROPOMI (b) tropospheric NO_2 vertical column densities (molecules cm^{-2}) for Domain 1 Texas (upper), Domain 3 Corpus Christi (middle), and Domain 4 San Antonio (lower). Data are averaged during 1 April–31 May at 0.1° × 0.1° resolution. (c) The differences between (a) and (b). (d) Regression between data shown in (a) and (b).

Discussion

As highlighted throughout this report, observations made during the field campaign broadly underscore the importance of off-shore activities for determining the composition of air being transported into the Corpus Christi atmosphere (e.g., off-shore sulfur emissions and biomass burning in Central America), meteorological influences on air quality (e.g., the land-sea breeze), and large differences in both composition and concentration of air pollutants across the spatial extent of the field campaign. Three-dimensional WRF-GC output shows that the model likely overpredicts background O_3 and underpredicts urban/vehicular emissions of NO_x and CO.

Other specific findings include:

a.) Trace gas concentrations are higher and more variable in San Antonio relative to Corpus Christi;

b.) San Antonio is likely impacted by more local and fresh emissions compared to Corpus Christi;

c.) Very low PM absorption coefficients were observed when the sampled air was representative of the marine boundary layer and after precipitation events compared to when air was influenced by combustion sources;

d.) VOC levels were influenced by biogenic compounds (monoterpenes and isoprene) throughout the study area;

e.) Formaldehyde exhibited strong diurnal trends in San Antonio;

f.) Variability in benzene, toluene, ethyl benzenes, and xylenes could be attributed partially to proximity to anthropogenic emission sources; and

g.) During transit from Corpus Christi to San Antonio, with respect to aerosol, sulfate mass and extent of OA oxidation decreased, while OA and nitrate mass, extent of neutralization, and influence of HOA and BBOA increased.

Future Work, Recommendations, and Concluding Remarks

Future work on this project will focus on continued data analysis, as well as development of related manuscripts for publication and platform talks/posters for presentation at national meetings. Specific items that will be pursued include:

a.) Continued evaluation of transport events (biomass burning, land/sea breeze, and synoptic versus mesoscale meteorological phenomena) and their influences on local air quality in the Corpus Christi-San Antonio greater urban areas and connecting corridor;
b.) Continued characterization of spatial differences in air quality between coastal and inland locations;
c.) Consideration of changes in air quality in San Antonio during the current campaign compared to that conducted in 2017, with a focus on determination of whether these changes are related to emissions control/changes, the COVID pandemic, and/or meteorology;
d.) Estimation of the relative influences of biogenic and anthropogenic VOC on O_3 and secondary fine PM (rather than simply total VOC level);
e.) Evaluation of mobile/local emissions by combining mobile sampling data and WRF-GC output (in light of the underestimation of CO and NO_X data on road); and
f.) Determination of a Corpus Christi air quality 'baseline' (i.e., background O_3) and a comparison to Houston.

Based on the preliminary findings from this very recent field campaign, several future field campaigns, each of which also could incorporate three-dimensional modeling activities and analysis of satellite data, appear necessary. These include a field campaign to determine the impact of offshore activities on air composition being transported into the Texas coast. This could include ship- and airplane-based measurements over the Gulf of Mexico. It also will be important to perform a seasonal comparison of air quality data such as those described in this report and those collected during the SAFS in 2017. The SAFS study was conducted in spring, and the original plan for the campaign described here was for a fall performance. The COVID pandemic necessitated the performance of this campaign in spring 2021. Therefore, a fall campaign in one or both of these locations will be an important future effort. Lastly, a large expansion of a refinery in Corpus Christi has received considerable attention in the public media. After this expansion, a campaign similar to that described in this report will allow for a 'before and after' comparison of air quality, allowing for inference of the impact of the refinery expansion on air pollution.

Work such as that described here is instrumental for understanding the chemical and physical processes that influence air quality at a given time and location, beyond that which is feasible using existing monitoring networks because of limitations in spatial and temporal resolution. The three-dimensional air quality modeling described here allows for additional insights related to emissions sensitivity and mesoscale meteorological phenomena. These two types of information are most useful and powerful when used in concert, such as in the project described here. The TCEQ should utilize these results to help design emissions control strategies to

minimize exposure of all citizens of Texas to harmful air pollution.